A Diffusion Tensor Resolution Phantom

M. Bach[1], B. Stieltjes[2], K. Fritzsche[3], W. Semmler[1], and F. B. Laun[1]
[1]Medical Physics in Radiology, German Cancer Research Center, Heidelberg, Germany, [2]Quantitative Imaging-based Disease Characterization, German Cancer Research Center, Heidelberg, Germany, [3]Medical Imaging and Biological Informatics, German Cancer Research Center, Heidelberg, Germany

Introduction

In recent years, there has been a remarkable progress in available diffusion phantoms that generate anisotropic diffusion. The proposed designs range from realistic replica of the human brain white matter [1], over phantoms mimicking fiber crossings [2-7], to phantoms providing high diffusion anisotropies as observed in principal white matter tracts [7,8]. However, a proper design for a resolution phantom is still lacking: the available phantom designs either do not provide a sufficiently well defined fiber bundle geometry [2-7,9], or the fiber bundles are thick strings of a centimeter diameter [7,8]. Therefore, the aim of this work was to construct and evaluate a geometrically well defined diffusion tensor resolution phantom.

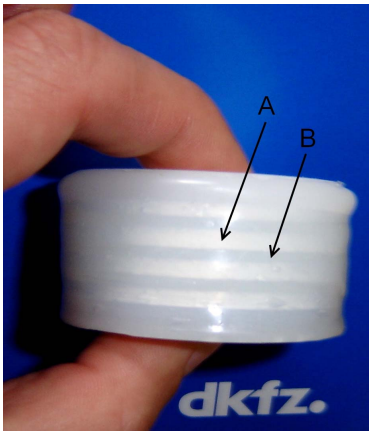

Fig. 1: DTI –Resolution-Phantom. **A**: fibers. **B**: polyamide

Materials and Methods

The phantoms consist of polyester fibers (15 µm) that are winded on a cylindrical polyamide spindle (Fig. 1). A sodium chloride solution (83 g NaCl per 1 l water) is embedded between the polyester fibers. This solution has the same susceptibility as polyester and minimizes mesoscopic B_0-field variations [8].
Four equal grooves of 2 mm thickness are cut in the spindle and the separation of two successive grooves is 2 mm. After winding, the phantom is sealed using hot glue. A sketch of the phantom is shown in Fig.2.
The phantom was measured on a 1.5 T MR scanner (Avanto, Siemens, Erlangen, Germany) with a twice refocused spin echo planar diffusion sequence. Parameters were: 30 slices, FOV = 200x100 mm^2, voxel size = 2x2x2 mm^3, TR = 3100 ms, TE = 77 ms, 32 averages, b = 0, 1000 s/mm^2. For the second measurement: 20 slices, FOV 300x150 mm^2, voxel size = 3x3x3 mm^3, TR = 3000 ms, TE = 66 ms, 32 averages, b = 0, 1000 s/mm^2.
Fiber tracking was performed with the free MedINRIA software, which uses tri-linear Log-Euclidean interpolation [10,11].

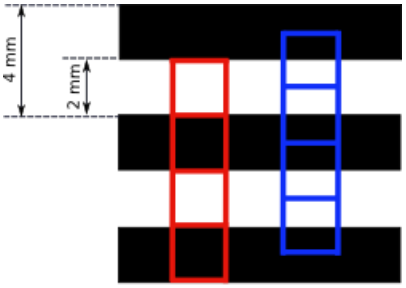

Fig. 2: Resolution phantom (schematic). Black: polyamide, white: fibers red and blue boxes: pixel positions

Results

Since the image resolution of the 2 mm voxels matched to the phantom groove spacing and thickness, two cases can be distinguished: Either the voxel locations overlap with the grooves (Fig. 2, red box), or they are located between the grooves (Fig. 2, blue box). Both cases can clearly be distinguished on the acquired fractional anisotropy (FA) maps (Fig. 3). In Fig. 3a, the grooves are clearly separated, while a clear separation is not possible if the image plane is shifted by 1 mm (Fig. 3b). The FA is about 0.7.
In Fig. 4, the obtained fiber tracking results are depicted for isotropic image resolutions of 2 mm (Fig. 4a) and 3 mm (Fig. 4b). The fibers strings are clearly separated in the 2 mm data set since the phantom was mostly well aligned with the imaging plane. In contrast, a separation of the fiber strings is not possible on the 3 mm data set.

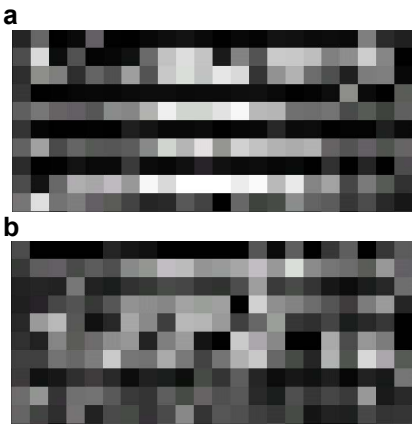

Fig.3: FA maps
a corresponding to the red box in Fig.2
b corresponding to the blue box in Fig.2

Discussion

The presented phantom geometry is well suited to perform resolution experiments and to validate fiber tracking algorithms under realistic conditions. For instance, the dependency of calculated tensor parameters and of reconstructed fibers on image resolution, signal-to-noise ratio, fiber orientation, parallel imaging method, or anisotropic voxel spacing can be evaluated and compared to theoretical results. Moreover, the effect of postprocessing schemes including voxel interpolation, filtering and denoising on the reconstructed data can be accessed. Future versions of the phantom will have a stronger outer wall to avoid deformations. In addition, the groove thickness can be varied.

References
[1] Delputte et al. ISMRM 2006 [2] Poupon, Philos Trans R Soc Lond B Biol Sci. 2005 [3] Watanabe et al. Rad. Med. 2006 [4] Poupon et al. MRM 2008 [5] Pullens ISMRM 2008 [6] Tournier et al. NeuroImage 2008 [7] Moussavi et al. MRM 2010 [8] Laun et al, MRI 2009 [9] Fieremans et al. J Magn Reson 2008 [10] P.Fillard et al. Proc. of MICCAI 2003 [11] V. Arsigny et al. MRM 2006

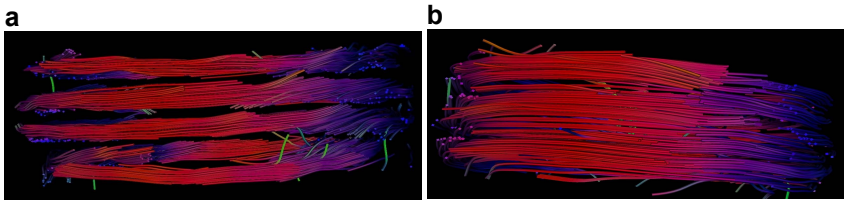

Fig.4 Fiber Tracking; voxel size: **a** isotropic 2 mm, **b** isotropic 3mm